Bond order instabilities in a correlated two-dimensional metal

Andrea Allais, Johannes Bauer, and Subir Sachdev
Department of Physics, Harvard University, Cambridge MA 02138
(Dated: April 4, 2014)

Motivated by recent experimental evidence of charge order in the pseudogap phase of cuprates, we perform a variational analysis of charge-neutral, spin-singlet ordering in metals on the square lattice, using a wavefunction with double occupancy projected out. We examine ordering with and without time-reversal symmetry, with arbitrary wavevector and tunable form factor. Depending on parameters, we find d-wave bond density wave ordering with wavevector either parallel to the lattice generators or diagonally oriented, or a ground state which carries a time reversal-breaking pattern of spontaneous currents.

There is growing experimental evidence that charge density wave order is a generic feature of underdoped cuprate high temperature superconductors. Its presence has been long established in La_2CuO_4 based compounds [1, 2]. In BSCCO, periodic modulations in the local density of states have been detected with STM, both in the mixed state near the vortex cores [3], and in the pseudogap state [4]. In $YBa_2Cu_3O_\gamma$, long range, static charge order has been detected with NMR [5, 6], and its effects show up in thermodynamic properties [7]. This order may explain the quantum oscillations seen in high magnetic field [8, 9]. At zero field, incommensurate charge order has been detected with resonant [10, 11] and hard [12] X-ray scattering. Collectively, the experiments point to the existence of incommensurate charge correlations in the CuO_2 plane, which are stabilized to static, long range order by a magnetic field, and in general compete with superconductivity. The wavevector is consistently found to be directed along the copper-oxygen bonds, and appears to be related to geometric properties of the Fermi surface [13] (Fig 1). There are also indications that the charge order lies predominantly on the *bonds* connecting the Cu sites [14–16].

Motivated by these remarkable experimental developments, we present a thorough exploration of charge density wave (CDW) instabilities in a strongly correlated, antiferromagnetic metal as described by a variational wavefunction in which doubly-occupied sites are projected out. Our main conclusions are that i) the antiferromagnetic interaction and electron correlations can cause the condensation of a d-wave CDW with the experimentally observed wavevector (we define a d-wave CDW as in Refs. [22, 23]—see below), a result that proved elusive so far under controlled approximations, and ii) for a different range of parameters, a state is favored which supports time-reversal breaking permanent currents, known in the literature as the staggered flux (SF) state [17–21].

From a theoretical point of view [22–32], a charge/bond density wave is a natural instability of a metal with antiferromagnetic interactions. This was explored in the context of a weak coupling analysis in Ref. 23, which showed that a bond-density wave arises with a wavevector $\boldsymbol{Q}$ and a local d-wave pattern of the bond modulations. Consistent with expectations, the wavevector $\boldsymbol{Q}$ was found to be very close to that connecting two hot spots on the Fermi surface (FS), which are points of the FS connected by the antiferromagnetic wavevector $\boldsymbol{K} = (\pi, \pi)$ (Fig. 1). However, the globally optimal wavevector was found to run diagonally. A restricted optimization for wavevectors parallel to the copper-oxygen bonds [23] (the wavevector direction observed in experiments) also yielded a wavevector close to that connecting hot spots (Fig. 1) and with a form factor which remained predominantly d-wave.

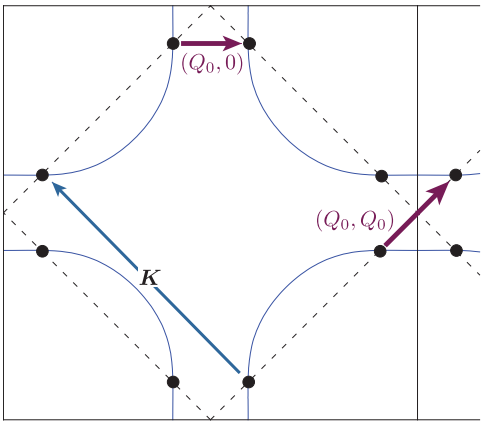

FIG. 1. Fermi surface with $t_1 = 1$, $t_2 = -0.32$, $t_3 = 0.128$, and $\mu = -1.11856$. For this dispersion we have $Q_0 = 4\pi/11$.

Here we show how strong electron correlations modify the picture above. We account for those Mott correlations variationally, using a Gutzwiller projected wavefunction which suppresses double occupancy of all sites [33–38]. We allow the condensation of a charge density waves with arbitrary wavevector and with tunable form factor (the form factors determines the intra-unit-cell structure of the density wave), as well as states which break time-reversal symmetry and carry different patterns of spontaneous currents. Among previously studied states, our study includes charged stripes [39], bond density waves [14, 40], Ising-nematic order [41–43], staggered flux states [17–21], and states with spontaneous currents [44]. Our main results are summarized below in Fig. 3:

we find regimes where the globally optimal state has a CDW with wavevector very close to $(Q_0, 0)$ and a d-wave form factor.

We consider the following model of a metal with antiferromagnetic and Coulomb interactions,

$$H = \sum_{\boldsymbol{x},\boldsymbol{a}} \Big[-t_a c^\dagger_{\boldsymbol{x}+\boldsymbol{a}} c_{\boldsymbol{x}} + \frac{J_a}{8} c^\dagger_{\boldsymbol{x}+\boldsymbol{a}} \vec{\sigma} c_{\boldsymbol{x}+\boldsymbol{a}} \cdot c^\dagger_{\boldsymbol{x}} \vec{\sigma} c_{\boldsymbol{x}} + \frac{V_a}{2} c^\dagger_{\boldsymbol{x}+\boldsymbol{a}} c_{\boldsymbol{x}+\boldsymbol{a}} c^\dagger_{\boldsymbol{x}} c_{\boldsymbol{x}} \Big] + H_U \,, \tag{1}$$

where the electrons c live on the sites $\boldsymbol{x}$ of a square lattice with spacing $a = 1$ and $\vec{\sigma}$ is the vector of Pauli matrices, which act on an implicit spin index. The vector $\boldsymbol{a}$ connects neighboring sites, and we allow first, second, and third neighbor hoppings t_1, t_2, t_3, respectively. However, we limit the Coulomb (V) and exchange (J) interactions to the nearest neighbors. H_U represents an infinite on-site Coulomb repulsion, which we account for by projecting out doubly occupied sites. The couplings are real and preserve all lattice symmetries, and we work at fixed density.

We seek to minimize the energy of the Hamiltonian (1) within the space of states

$$|\text{var}\rangle \equiv \left[\prod_i (1 - n_{i\uparrow} n_{i\downarrow}) \right] |\text{gd}(H_{\text{var}})\rangle \,, \tag{2}$$

where $|\text{gd}(H_{\text{var}})\rangle$ is the ground state of the quadratic hamiltonian

$$H_{\text{var}} = \sum_{\boldsymbol{x},\boldsymbol{a}} \left[-T_{\boldsymbol{a}} + \phi_{\boldsymbol{a}} \cos \boldsymbol{Q} \cdot (\boldsymbol{x} + \boldsymbol{a}/2) \right] c^\dagger_{\boldsymbol{x}+\boldsymbol{a}} c_{\boldsymbol{x}} \,, \tag{3}$$

and the state $|\text{var}\rangle$ has no doubly occupied sites by construction. $T_{\boldsymbol{a}}$ are variational hopping parameters and $\phi_{\boldsymbol{a}}$ parameters for the ordering wave-function. We note that the particular parameterization in Eq. (3) is carefully chosen [22, 23]: it is crucial that $\boldsymbol{Q}$ couple to the center-of-mass co-ordinate of the particle-hole pair for an efficient symmetry characterization of order parameters at incommensurate $\boldsymbol{Q}$. Previous analyses [19, 40, 45] did not make this choice.

This variational ansatz allows for the condensation of a charge/bond density wave with wavevector $\boldsymbol{Q}$, whose local pattern (the form factor) is determined by the wavefunction ϕ. That is,

$$\left\langle c^\dagger_{\boldsymbol{x}+\boldsymbol{a}} c_{\boldsymbol{x}} \right\rangle_{\text{var}} = -\bar{T}_{\boldsymbol{a}} + \bar{\phi}_{\boldsymbol{a}} \cos \left[\boldsymbol{Q} \cdot (\boldsymbol{x} + \boldsymbol{a}/2) \right] \,, \tag{4}$$

where $\bar{\phi}$ is nonzero if and only if ϕ is nonzero, and they both have the same symmetries under point group transformations and time reversal. We further restrict $\phi_{\boldsymbol{a}}$ to have the form

$$\begin{aligned} \phi_{\boldsymbol{a}} = P_1 \delta_{\boldsymbol{a}} + \;& P_2 (\delta_{\boldsymbol{a}-\hat{\boldsymbol{x}}} + \delta_{\boldsymbol{a}-\hat{\boldsymbol{y}}} + \delta_{\boldsymbol{a}+\hat{\boldsymbol{x}}} + \delta_{\boldsymbol{a}+\hat{\boldsymbol{y}}}) \\ + \;& P_3 (\delta_{\boldsymbol{a}-\hat{\boldsymbol{x}}} - \delta_{\boldsymbol{a}-\hat{\boldsymbol{y}}} + \delta_{\boldsymbol{a}+\hat{\boldsymbol{x}}} - \delta_{\boldsymbol{a}+\hat{\boldsymbol{y}}}) \\ + \;& \mathrm{i}\, P_4 (\delta_{\boldsymbol{a}+\hat{\boldsymbol{x}}} + \delta_{\boldsymbol{a}-\hat{\boldsymbol{y}}} - \delta_{\boldsymbol{a}+\hat{\boldsymbol{x}}} - \delta_{\boldsymbol{a}+\hat{\boldsymbol{y}}}) \\ + \;& \mathrm{i}\, P_5 (\delta_{\boldsymbol{a}-\hat{\boldsymbol{x}}} - \delta_{\boldsymbol{a}-\hat{\boldsymbol{y}}} - \delta_{\boldsymbol{a}+\hat{\boldsymbol{x}}} + \delta_{\boldsymbol{a}+\hat{\boldsymbol{y}}}) \,, \end{aligned} \tag{5}$$

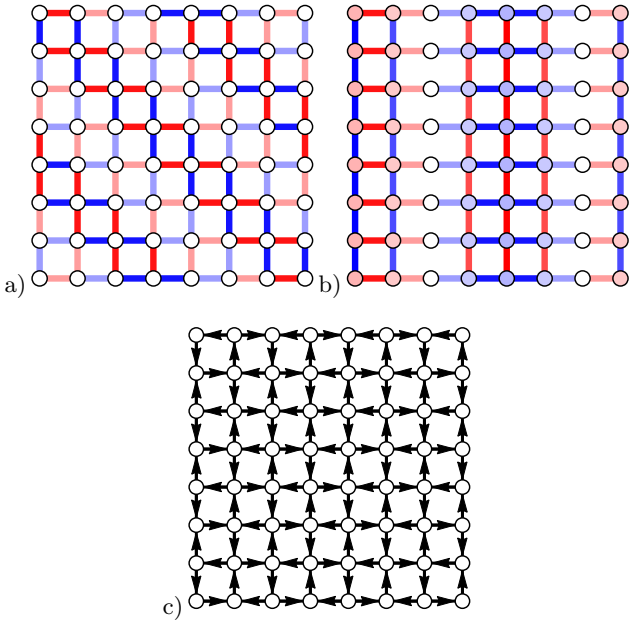

FIG. 2. Schematic illustration of the ordering patterns in real space. a) diagonal d-wave CDW ($P_3 \neq 0$, $\boldsymbol{Q} = (0.25, 0.25)\pi$) b) horizontal, predominantly d-wave CDW ($P_3 \neq 0$, $\boldsymbol{Q} = (0.25, 0)\pi$) c) staggered flux state ($P_5 \neq 0$, $\boldsymbol{Q} = (\pi, \pi)$). For the time reversal invariant orders a) and b) we show the fluctuation of $\langle c^\dagger_{\boldsymbol{x}+\boldsymbol{a}} c_{\boldsymbol{x}} \rangle$ about the average with positive (red) and negative (blue) values. For the time reversal breaking order c) we show the pattern of permanent currents.

with $\hat{\boldsymbol{x}} = (1, 0)$, $\hat{\boldsymbol{y}} = (0, 1)$. Time reversal is preserved if $P_4 = P_5 = 0$. If $P_1, P_2 \gg P_3$, a predominantly s-wave charge/bond density wave is induced, whereas $P_1, P_2 \ll P_3$ induces a predominantly d-wave bond density wave. It is important to notice that, for generic $\boldsymbol{Q}$, s- and d-wave characters mix, so that $P_3 = 0$ does not imply that $\bar{\phi}_{\boldsymbol{a}}$ is purely s-wave. If P_4 or P_5 are nonzero, a time reversal breaking pattern of spontaneous currents is created. In particular the state with only $P_5 \neq 0$ and $\boldsymbol{Q} = (\pi, \pi)$ is the staggered flux state. Figure 2 shows a schematic representation of a few relevant CDW and spontaneous current patterns.

We carry out the variational computation in a slightly unusual way. Ideally, we would like to prescribe, and keep fixed, the Fermi surface of the system, especially the presence and location of hot spots. This is the Fermi surface seen in, say, photoemission experiments, and it is different from the one obtained from the kinetic term in (1), because of interaction effects. This "true" Fermi surface is not easily accessible, but the Fermi surface of the optimal variational Hamiltonian is a close proxy. Therefore, instead of minimizing with respect to the variational hoppings T_a, we set them to values of our satisfaction, and tune the bare hoppings t_a in such a way as to make our choice a variational optimum [30]. We carry out this procedure while having all $P_i = 0$, then we look at what

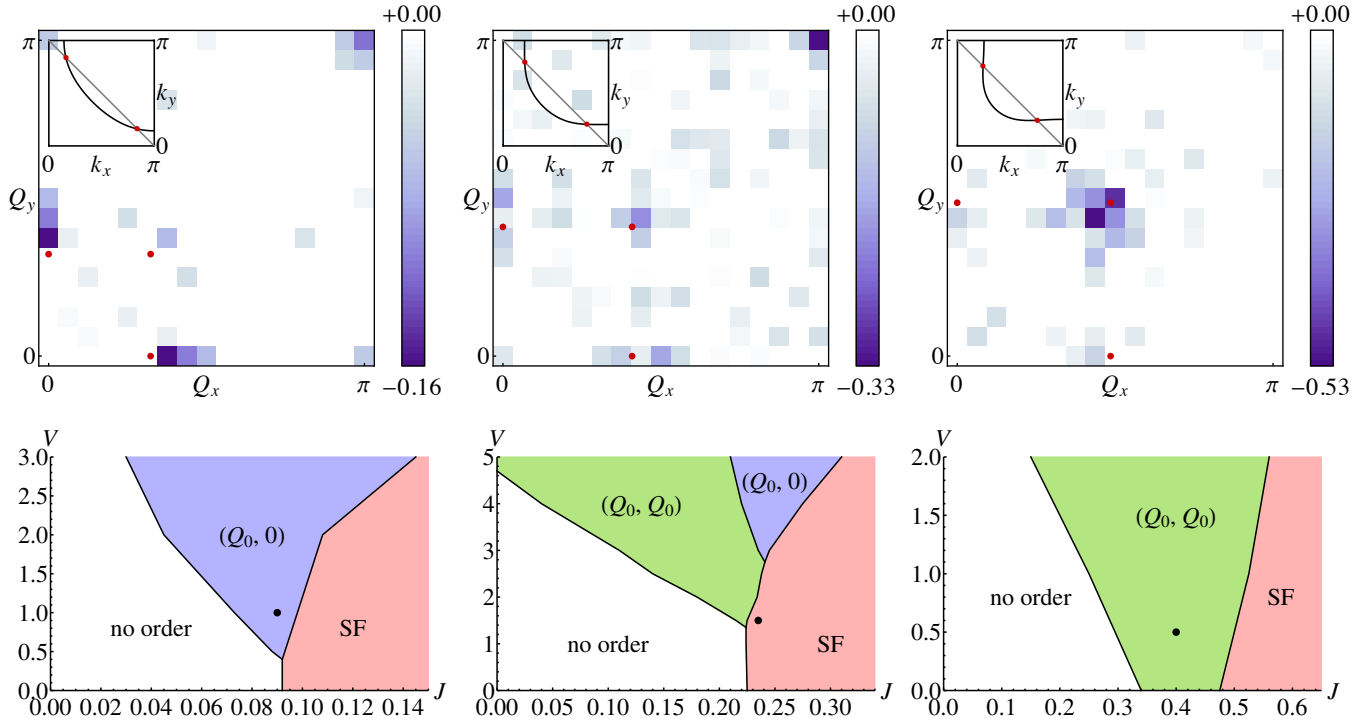

FIG. 3. In the top row, the gain in variational energy (per site, times 100) by allowing ordering at wavevector $\boldsymbol{Q}$ is displayed. Each diagram is for a different Fermi surface, shown in the inset. The local minimum at $\boldsymbol{Q} = (\pi, \pi)$ is the staggered flux state $P_5 \neq 0$. The local minima at $\boldsymbol{Q} = (Q_0, Q_0)$ and $\boldsymbol{Q} = (Q_0, 0)$ are predominantly d-wave CDW ($P_3 \neq 0$). The red dots denote wavevectors $\boldsymbol{Q}$ that connect hot spots. In the bottom row, we show approximate diagrams of the ground state order, as a function of J and V. The setup corresponding to the plot above is indicated with a black dot. Model parameters (values in the brackets correspond to plots from left to right): $x = 10\%$, $t_1 = 1$, $t_2 \in \{0.5, 0.16, 0.18\}$, $t_3 \in \{0.6, 0.9, 1.6\}$, $J \in \{0.09, 0.235, 0.4\}$, $V \in \{1., 1.5, 0.5\}$. Variational parameters: $T_1 = 1.$, $T_2 \in \{-0.1, -0.32, -0.5\}$, $T_3 = 0.128$. As described in the text the Fermi surface is determined by the T_a parameters.

CDW order can further improve the variational bound, while keeping T_a fixed. For each wavevector $\boldsymbol{Q}$, we minimize the variational energy, $\langle \text{var}| H |\text{var}\rangle$, with respect to the parameters P_i, one at a time. For a few choice wavevectors $\boldsymbol{Q}$ we also looked at simultaneous minimization with respect to P_1, P_2 and P_3, without finding significant additional energy gains. This three parameter minimization is the limit of the computational resources at our disposal.

In order to have sufficient momentum resolution, we use a lattice of 32×32 sites. Because the wavefunction is not a smooth function of the variational parameters, we cannot use derivative information to carry out the minimization, so we compute the energy over a grid of points in variational space. More precisely, we store the expectation value of every operator making up the Hamiltonian (1). This allows us to explore the parameter space without having to recompute the energy for every setup. Our grid comprises a total of about 30,000 points in variational space, each point requiring about 12 hr of CPU time on a 1.7GHz AMD Opteron.

Fig. 3 illustrates the results of this variational analysis. For a few representative choices of model parameters, we show the $\boldsymbol{Q}$ values the system finds it energetically favorable to order. The form factor corresponding to each energy minimum is not explicitly shown in the plot. The minimum at $\boldsymbol{Q} = (\pi, \pi)$ has $P_5 \neq 0$, i.e. it is the SF state, whereas all other minima are predominantly d-wave CDW, i.e. have $P_3 \neq 0$. The parameters are chosen close to the onset of the order. A more comprehensive picture is given by the approximate phase diagrams of the bottom row, which show the kind of order that yields the greatest gain in energy over a range of parameters. The staggered flux state is dominant at large J, but is suppressed by the Coulomb repulsion V which prefers CDWs. As can be seen in the upper row, in addition to this main order, other subleading energy minima are usually present. In particular, even when the global energy minimum is the staggered flux state, the CDWs are still present as a local minimum. The CDWs become global minima at smaller J, and the appropriate Fermi surface configuration and moderate J stabilize the wavevector $\boldsymbol{Q} = (Q_0, 0)$ over $\boldsymbol{Q} = (Q_0, Q_0)$. In our framework, we cannot address the issue of competition between orders, as this would require simultaneous minimization with respect to several more parameters, but

we expect that the $\boldsymbol{Q} = (Q_0, 0)$ CDW can coexist with the staggered flux state, since their mixing is prevented by time-reversal symmetry.

Our computations have shown that the observed charge order with $\boldsymbol{Q}$ along the copper-oxygen bonds appears over a regime of parameters in a variational computation of a correlated metal with antiferromagnetic interactions. The magnitude of $\boldsymbol{Q}$ is close to that determined by the antiferromagnetic hot spots (Fig. 1), and its form factor was robustly found to be predominantly d-wave (defined as in Refs. [22, 23]).

After our study was complete, we learnt of the related study of Ref. [46] addressing symmetry breaking in the superconductor, rather than the metal, in a model with only nearest-neighbor hopping.

We also note recent experimental reports [47, 48] concluding that the charge order at $(Q_0, 0)$ is predominantly d-wave, as discussed above.

We thank D. Chowdhury, A. Georges, and J. Sau for valuable discussions. The research was supported by the U.S. National Science Foundation under grant DMR-1103860, and by the Templeton Foundation. JB acknowledges financial support from the DFG through grant number BA 4371/1-1. The simulation was done on the MIT LNS Tier 2 cluster.

[1] J. Tranquada *et al.* Nature **375**, 561 (1995).
[2] P. Abbamonte *et al.* Nature Physics **1**, 155 (2005).
[3] J. Hoffman *et al.* Science **295**, 466 (2002).
[4] M. Vershinin *et al.* Science **303**, 1995 (2004).
[5] T. Wu *et al.*, Nature **477**, 191 (2011).
[6] T. Wu *et al.*, Nature Comm. **4**, 2113 (2013).
[7] D. LeBoeuf, S. Krämer, W. N. Hardy, Ruixing Liang, D. A. Bonn, and C. Proust, Nature Physics **9**, 79 (2013).
[8] N. Doiron-Leyraud *et al.* Nature **447** 565 (2007).
[9] S. Sebastian, N. Harrison, and G.G. Lonzarich, Rep. Prog. Phys. **75** 102501 (2012).
[10] G. Ghiringhelli *et al.*, Science **337**, 821 (2012).
[11] A. J. Achkar *et al.*, Phys. Rev. Lett. **109**, 167001 (2012).
[12] J. Chang *et al.*, Nature Phys. **8**, 871 (2012).
[13] R. Comin *et al.* Science **343** 390 (2013).
[14] S. Sachdev, Rev. Mod. Phys. **75**, 913 (2003).
[15] Y. Kohsaka *et al.*, *Science* **315**, 1380 (2007).
[16] A. J. Achkar *et al.*, Phys. Rev. Lett. **110**, 017001 (2013).
[17] I. Affleck and J. B. Marston, Phys. Rev. B **37**, 3774 (1988).
[18] Z. Wang, G. Kotliar, and X.-F. Wang, Phys. Rev. B **42**, 8690 (1990).
[19] S. Chakravarty, R. B. Laughlin, D. K. Morr, and C. Nayak, Phys. Rev. B **63**, 094503 (2001).
[20] P. A. Lee, N. Nagaosa, and X.-G. Wen, Rev. Mod. Phys. **78**, 17 (2006).
[21] R. B. Laughlin, Phys. Rev. B **89**, 035134 (2014).
[22] M. A. Metlitski and S. Sachdev, Phys. Rev. B **82**, 075128 (2010).
[23] S. Sachdev and R. La Placa, Phys. Rev. Lett. **111**, 027202 (2013).
[24] T. Holder and W. Metzner, Phys. Rev. B **85**, 165130 (2012); C. Husemann and W. Metzner, Phys. Rev. B **86**, 085113 (2012).
[25] M. Bejas, A. Greco, and H. Yamase, Phys. Rev. B **86**, 224509 (2012).
[26] K. B. Efetov, H. Meier, and C. Pépin, Nature Physics **9**, 442 (2013).
[27] Hae-Young Kee, C. M. Puetter, and D. Stroud, J. Phys.: Condens. Matter **25**, 202201 (2013).
[28] S. Bulut, W. A. Atkinson, and A. P. Kampf, Phys. Rev. B **88**, 155132 (2013).
[29] J. C. Séamus Davis and Dung-Hai Lee, Proc. Natl. Acad. Sci. **110**, 17623 (2013).
[30] J. D. Sau and S. Sachdev, Phys. Rev. B **89**, 075129 (2014).
[31] H. Meier, C. Pépin, M. Einenkel, and K. B. Efetov, arXiv:1312.2010.
[32] Yuxuan Wang and A. V. Chubukov, arXiv:1401.0712.
[33] M. Gutzwiller, Phys. Rev. Lett. **10**, 159 (1963).
[34] C. Gros, Ann. Phys. **189**, 53 (1989).
[35] A. Paramekanti, M. Randeria and N. Trivedi, Phys. Rev. Lett. **87**, 217002 (2001) and Phys. Rev. B **70**, 054504 (2004).
[36] M. Raczkowski, D. Poilblanc, R. Frésard, and A. M. Oleś, Phys. Rev. B 75, 094505 (2007).
[37] S. Pathak, V. B. Shenoy, M. Randeria, and N. Trivedi, Phys. Rev. Lett. **102**, 027002 (2009).
[38] R. Sensarma and V. Galitski, Phys. Rev. B **84**, 060503(R) (2011).
[39] S. A. Kivelson, I. P. Bindloss, E. Fradkin, V. Oganesyan, J. M. Tranquada, A. Kapitulnik, and C. Howald, Rev. Mod. Phys. **75**, 1201 (2003).
[40] M. Vojta and O. Rösch, Phys. Rev. B **77**, 094504 (2008).
[41] H. Yamase and H. Kohno, J. Phys. Soc. Jpn. **69**, 2151 (2000).
[42] C. J. Halboth and W. Metzner, Phys. Rev. Lett. **85**, 5162 (2000).
[43] V. Oganesyan, S. A. Kivelson, and E. Fradkin, Phys. Rev. B **64**, 195109 (2001).
[44] M. E. Simon and C. M. Varma, Phys. Rev. Lett. **89**, 247003 (2002).
[45] C. Nayak, Phys. Rev. B **62**, 4880 (2000).
[46] P. Corboz, T. M. Rice, and M. Troyer, arXiv:1402.2859.
[47] R. Comin *et al.*, arXiv:1402.5415.
[48] K. Fujita *et al.*, arXiv:1404.0362.